Supplementary Material

Engineered Hybrid Cell Membrane Nanovesicles for Potentiated Cancer Immunotherapy through Dual Immune Checkpoint Inhibition

Fuxu Yang[a,b#], Han Xue[b#], Yuxin Fan[b#], Ting Zhang[a], Ting Wang [a], Fanlin Gu[b], Longxue Guan[b], Lisha Zhou[a,*], Xingang Guan[a,*] Guofu Chen[a,*]

[a] The First People's Hospital of Wenling (Taizhou University Affiliated Wenling Hospital), School of Medicine, Taizhou University, Taizhou 317500, PR China

[b] College of Medical Technology, Beihua University, Jilin 132013, PR China

Corresponding authors: lishazhou@tzc.edu.cn (L. Zhou); guanxg@ciac.ac.cn (X. Guan), wlcgf@163.com (G. Chen).

[#] These authors contribute to this work equally.

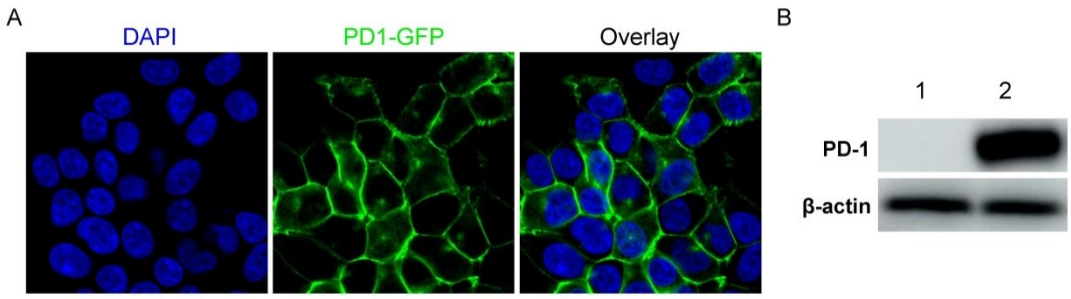

Figure S1. CLSM imaging (A) and western blot analysis (B) of PD-1-GFP stable cell lines. The nucleus was stained with DAPI (indicated in blue), and the PD-1 receptor was represented in green. Total protein from HEK-293T cells or HEK-293T-PD-1 cells was used for western blot analysi. Antibodies targeting mouse PD-1 was used.

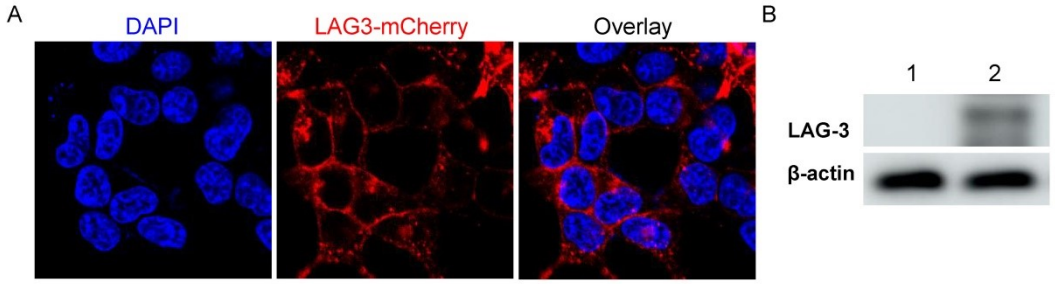

Figure S2. CLSM imaging (A) and western blot analysis (B) of LAG-3-mCherry stable cell lines. The nucleus was stained with DAPI (indicated in blue), and the LAG-3 receptor was represented in red. Total protein from HEK-293T cells or HEK-293T-LAG-3 cells was used for western blot analysi. Antibodies targeting mouse LAG-3 was used.

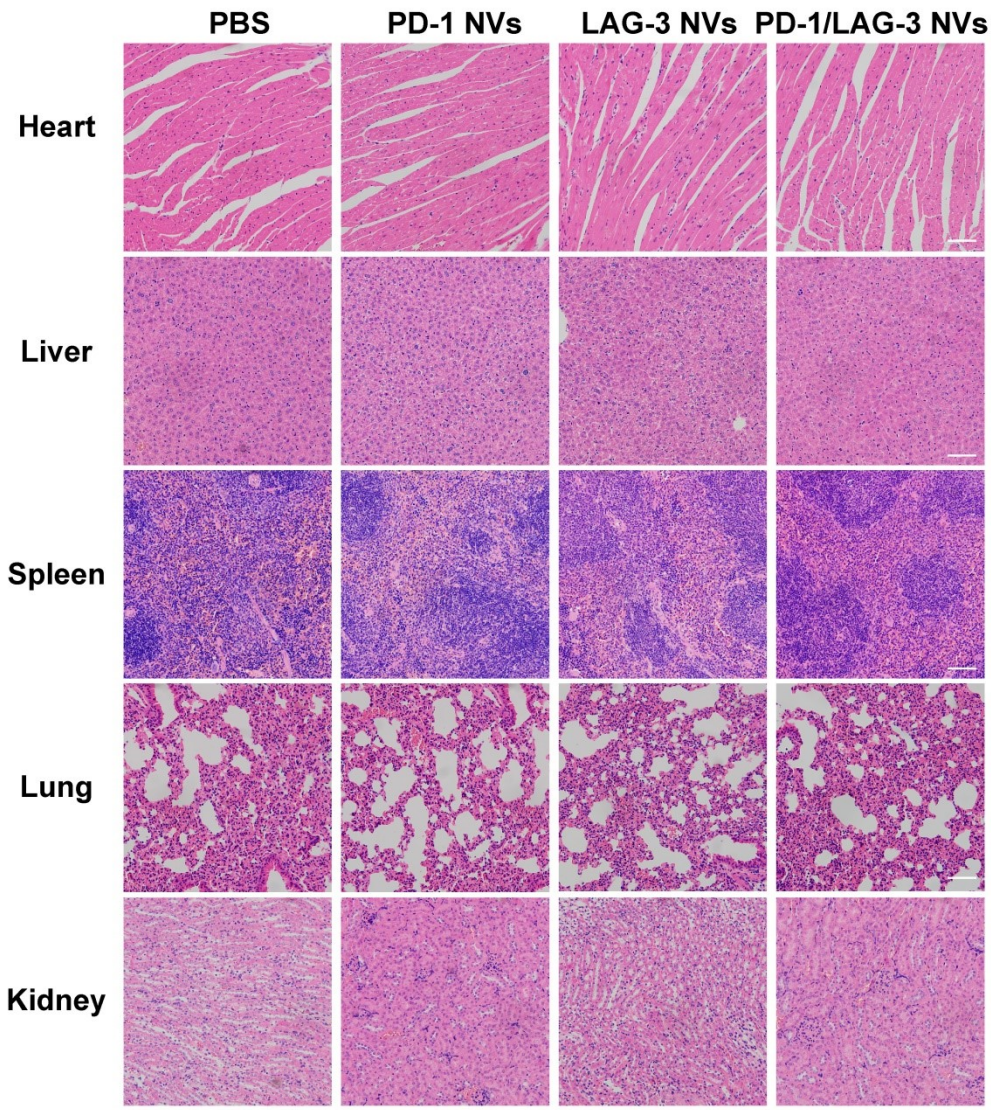

Figure S3. Histological images for H&E staining obtained from the liver, spleen, kidney, heart, and lung of mice with different treatments. Scale bar: 100 μm.

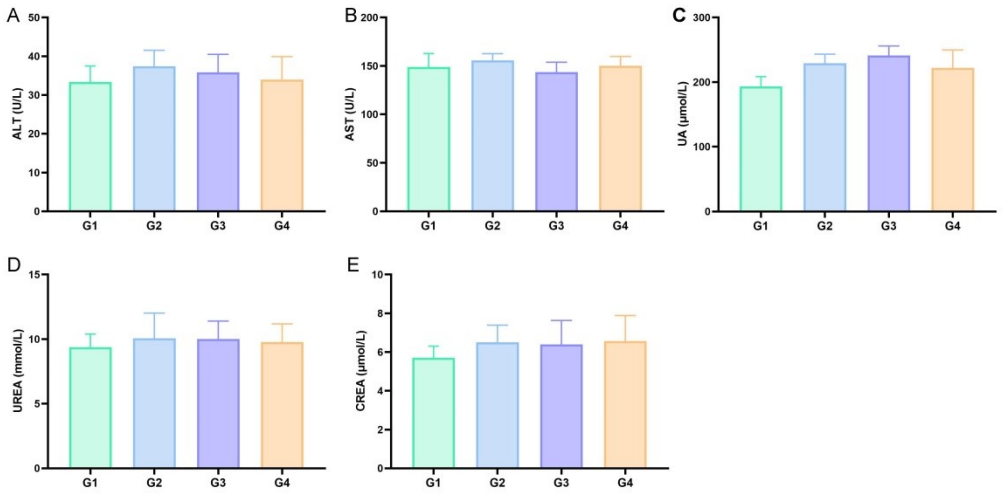

Figure S4. Serum biochemical analysis of kidney and liver function parameters. Data are expressed as mean ± SD (n=3). The levels of ALT (Figure S8A), AST (Figure S8B), UA (Figure S8C), Urea (Figure S8D), and Crea (Figure S8E) in the supernatants were determined.

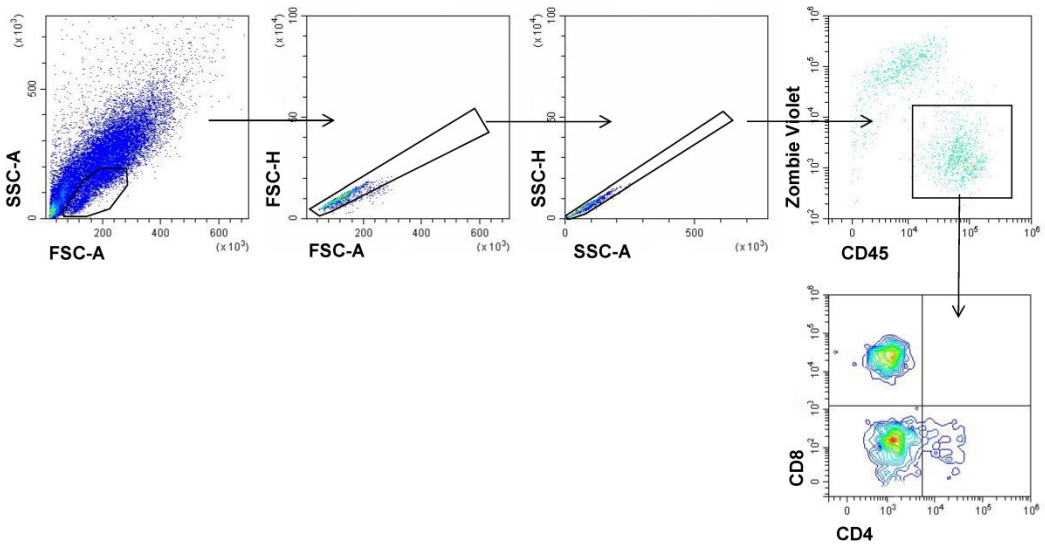

Figure S5. Flow cytometry gating strategies for $CD8^+$ T cells in tumors. The cells were gated for positive $CD45^+CD8^+$ expression.

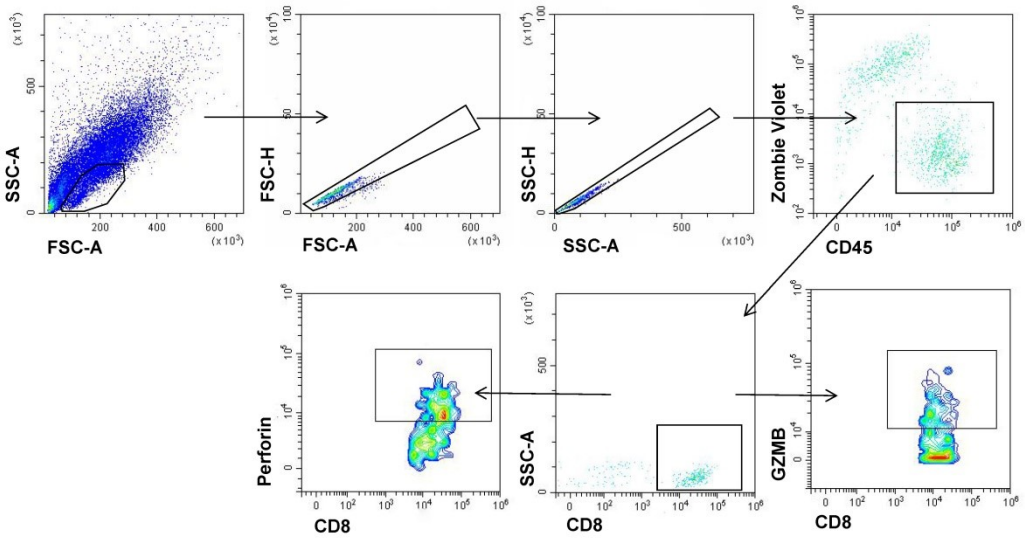

Figure S6. Flow cytometry gating strategies for perforin or GZMB positive $CD8^+$ T cells in tumors. The cells were gated for positive $CD45^+CD8^+$ expression.

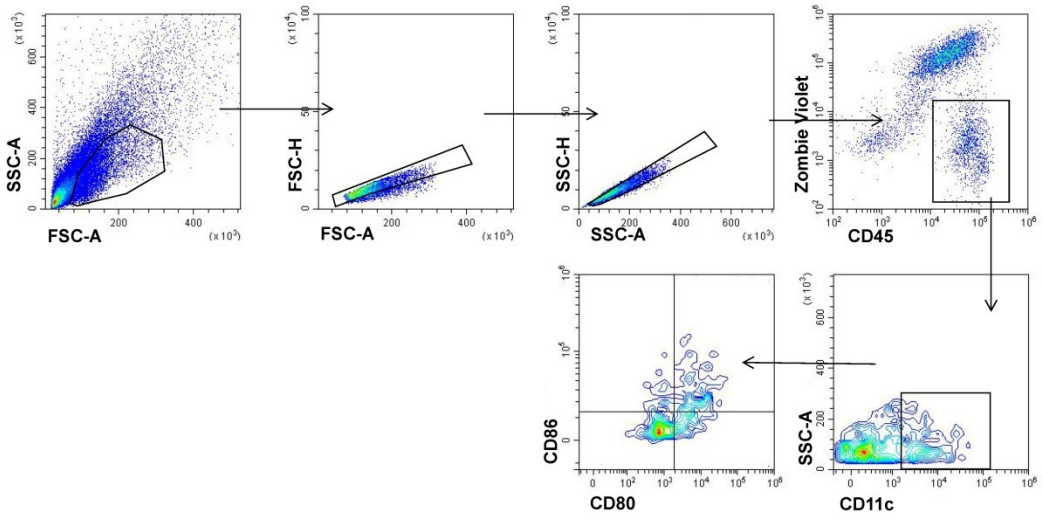

Figure S7. Flow cytometry gating strategies for dendritic cells in tumors. The cells were gated for positive $CD80^+CD86^+$ expression.

Figure S8. Flow cytometry gating strategies for Treg cells in tumors. The cells were gated for positive $CD45^+CD4^+Foxp3^+$ expression.

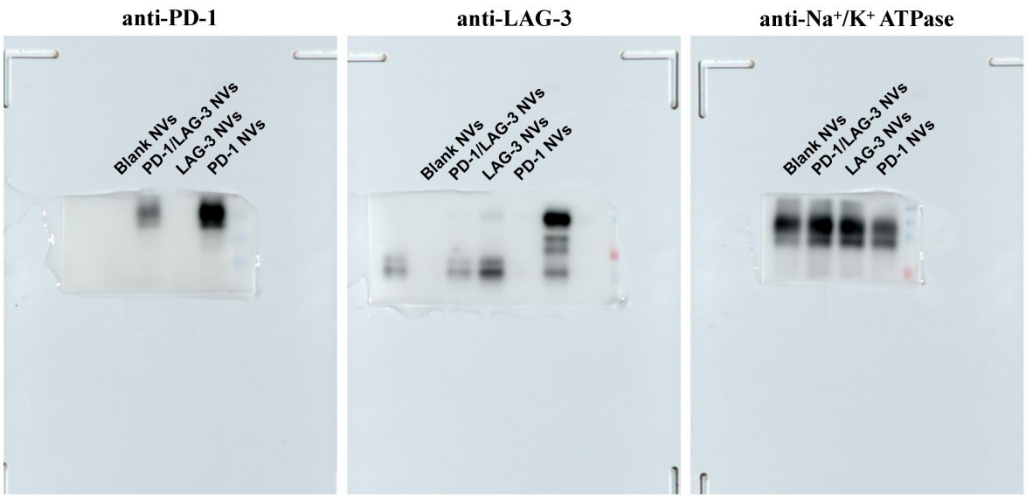

Figure S9. Uncropped and unprocessed images used in Figure 2B in this study.